Published OnlineFirst January 15, 2015; DOI: 10.1158/0008-5472.CAN-14-1643

Microenvironment and Immunology

Cancer Research

ERAP1 Regulates Natural Killer Cell Function by Controlling the Engagement of Inhibitory Receptors

Loredana Cifaldi[1], Paolo Romania[1], Michela Falco[2], Silvia Lorenzi[1], Raffaella Meazza[3], Stefania Petrini[4], Marco Andreani[5], Daniela Pende[3], Franco Locatelli[1,6], and Doriana Fruci[1]

Abstract

The endoplasmic reticulum aminopeptidase ERAP1 regulates innate and adaptive immune responses by trimming peptides for presentation by MHC class I (MHC-I) molecules. Herein, we demonstrate that genetic or pharmacological inhibition of ERAP1 on human tumor cell lines perturbs their ability to engage several classes of inhibitory receptors by their specific ligands, including killer cell Ig-like receptors (KIR) by classical MHC-I–peptide (pMHC-I) complexes and the lectin-like receptor CD94-NKG2A by nonclassical pMHC-I complexes, in each case leading to natural killer (NK) cell killing. The protective effect of pMHC-I complexes could be restored in ERAP1-deficient settings by the addition of known high-affinity peptides, suggesting that ERAP1 was needed to positively modify the affinity of natural ligands. Notably, ERAP1 inhibition enhanced the ability of NK cells to kill freshly established human lymphoblastoid cell lines from autologous or allogeneic sources, thereby promoting NK cytotoxic activity against target cells that would not be expected because of KIR–KIR ligand matching. Overall, our results identify ERAP1 as a modifier to leverage immune functions that may improve the efficacy of NK cell–based approaches for cancer immunotherapy. *Cancer Res; 75(5); 824–34. ©2015 AACR.*

Introduction

Natural killer (NK) cells provide the first innate immune defense against infections and malignancies through direct recognition and killing of altered cells (1, 2).

NK cell function is finely tuned by the interaction of activating and inhibitory receptors with their specific ligands expressed on target cells (3). Activating receptors recognize ligands on stressed, infected (4, 5), or transformed cells (6, 7), whereas inhibitory receptors, represented by killer cell Ig-like receptors (KIR) and CD94-NKG2A in humans (8–10) and Ly49 in mice (11), bind MHC-I molecules expressed on target cells (12). Downregulation of ligands for inhibitory receptors ("missing self-recognition") and upregulation of ligands for activating receptors ("induced self-recognition") in both virally infected and transformed cells make these cells particularly vulnerable to NK cell killing.

NK cells undergo an educational process that ensures the selection of a functional self-tolerant NK cell repertoire during development. The acquisition of NK cell full function relies on the binding of MHC-I molecules to the specific inhibitory KIRs, a mechanism that is referred to as NK cell "licensing" or "education" (13–16).

Inhibitory receptors recognize specific groups of classical and nonclassical MHC-I alleles. In general, KIR2DL1 binds HLA-C alleles with lysine at position 80 (group 2 or C2); KIR2DL2 and KIR2DL3 bind HLA-C alleles with asparagine at position 80 (group 1 or C1); KIR3DL1 recognizes HLA-B and HLA-A alleles expressing Bw4 epitope; KIR3DL2 recognizes HLA-A*03 and HLA-A*11, whereas CD94-NKG2A receptor interacts with nonclassical MHC-Ib HLA-E molecule (9, 10, 17).

KIRs recognize their ligands through the direct contact with MHC-I heavy-chain residue at position 80 (18, 19) and amino acid residues 7 and 8 of the bound peptide (20, 21), whereas the CD94-NKG2A receptor interacts with amino acid residues 5, 6, and 8 of peptide bound to HLA-E molecules (22). Residues at these positions have been shown to either promote or abrogate binding of inhibitory receptors (23, 24). Because all inhibitory receptors tested so far exhibit selectivity for peptides bound to MHC-I molecules (25), it is possible that modifications of peptides presented by MHC-I interfere with NK cell inhibition.

Molecules known as ERAAP in mice (26) and ERAP1 and ERAP2 in humans (27–29) are key components of the antigen trimming machinery in the endoplasmic reticulum (ER). We have recently shown that in mice, the abrogation of ERAAP induces a conformational change in the peptide–MHC-I (pMHC-I) complexes, resulting in the stimulation of both innate and adaptive immune responses and in the rejection of a murine lymphoma, which is otherwise refractory to immune elimination (30). However, it is not known whether human ERAP1 inhibition might

[1]Paediatric Haematology/Oncology Department, IRCCS, Ospedale Pediatrico Bambino Gesù, Rome, Italy. [2]Istituto Giannina Gaslini, IRCCS, Genoa, Italy. [3]IRCCS AOU San Martino-IST, Genoa, Italy. [4]Research Laboratories, Confocal Microscopy Core Facility, IRCCS, Ospedale Pediatrico Bambino Gesù, Rome, Italy. [5]Laboratory of Immunogenetics and Transplant Biology, IME Foundation, Polyclinic of Tor Vergata, Rome, Italy. [6]University of Pavia, Pavia, Italy.

Note: Supplementary data for this article are available at Cancer Research Online (http://cancerres.aacrjournals.org/).

Corresponding Authors: Doriana Fruci, Immuno-Oncology Laboratory, Paediatric Haematology/Oncology Department, Bambino Gesù Children's Hospital, IRCCS, Viale di San Paolo 15, Rome 00146, Italy. Phone: 39-06-6859-2657; Fax: 39-06-6859-2904; E-mail: doriana.fruci@opbg.net; and Franco Locatelli, franco.locatelli@opbg.net.

doi: 10.1158/0008-5472.CAN-14-1643

Published OnlineFirst January 15, 2015; DOI: 10.1158/0008-5472.CAN-14-1643

affect immune responses against tumors, and therefore represent a new tool to improve NK cell–based anticancer therapy protocols.

To address this issue, we stably reduced ERAP1 function in a panel of human cell lines either by genetic or pharmacological inhibition. We show that inhibition of ERAP1 renders DAOY cells susceptible to NK cell killing due to a poor recognition of pMHC-I complexes by KIRs (KIR2DL1, KIR2DL3, and KIR3DL1) and CD94-NKG2A receptor. Of note, inhibition of ERAP1 enhanced NK cell killing of lymphoblastoid cell lines (LCL) in both alloreactive and nonalloreactive settings, regardless of the presence of KIR–KIR ligand matching.

Materials and Methods

Cell lines and reagents

All human tumor cell lines were obtained from the ATCC and characterized every 6 months by HLA class I typing (Supplementary Table S1). EBV-transformed LCLs were generated from healthy donors using standard procedures. RPMI-8866 cell line was kindly provided by A. Santoni (La Sapienza, University of Rome, Rome, Italy). All cells were maintained in RPMI-1640 medium supplemented with 10% FCS (Gibco), 300 μg/mL glutamine, 100 μg/mL penicillin, and 50 μg/mL streptomycin. For Leu-SH treatment, cells were cultured for 18 hours with 30 or 100 μmol/L/0.5 mmol/L Leu-SH/DTT (Sigma-Aldrich). Synthetic peptides used were from ProImmune (Supplementary Table S2).

Lentiviral infection

Lentiviral particles were generated in HEK293T cells by combining a pLKO.1 plasmid containing shRNA sequences, packaging plasmid pCMV-dR8.74, and envelope plasmid VSV-G/pMD2.G. Tumor cells were infected by the spin inoculation method with lentivirus containing a nontarget shRNA control vector (SHC002) or either of the ERAP1 shRNAs (clone ID: TRCN0000060539, TRCN0000060540, TRCN0000060541, and TRCN0000060542) targeting different sequences of human ERAP1 (Sigma-Aldrich).

HLA and KIR genotyping

Genomic DNA was extracted using the QIAamp DNA Blood Mini Kit (Qiagen). Low- and high-resolution typing for HLA-A, -B, and -C loci were performed by PCR sequence–specific oligonucleotides (PCR-SSO; Luminex) and PCR sequence–specific primers (PCR-SSP; Olerup), respectively. The KIR gene profiles were performed using the Olerup SSP KIR Genotyping Kit (GenoVision). Supplementary Tables S1, S3–S6 show the complete profiles of HLA class I and KIR loci.

KIR-binding assay

DAOY cells were stained with KIR–Fc fusion proteins KIR2DL1–Fc, KIR2DL3–Fc, and KIR3DL1–Fc (R&D Systems) for 1 hour at 4°C followed by phycoerythrin-conjugated goat $F(ab')_2$ anti-human IgG antibody (Molecular Probes), and then analyzed by flow cytometry.

Peptide loading on MHC class I molecules

The dissociation of preformed pMHC-I complexes and replacement of high-affinity peptides were performed as previously described (31). Peptide-pulsed cells were stained with mAb W6/32 and analyzed by flow cytometry, or used as target cells for NK cell degranulation assay.

Human NK cell isolation

In some experiments, human NK cells were isolated from peripheral blood mononuclear cells (PBMC) of healthy donors with the RosetteSep NK cell enrichment mixture method (StemCell Technologies) and Ficoll-Paque Plus (Amersham) centrifugation. NK cells with purity greater than 90% were stimulated with 100 IU/mL of recombinant human IL2 (PeproTech) for 18 hours at 37°C. To analyze NK cell degranulation on KIR single–positive or NKG2A single–positive subsets, purified NK cells were activated and expanded as previously described (Supplementary Methods; ref. 32). Otherwise, polyclonal NK cell cultures were obtained by coculturing nonadherent human PBMCs from buffy coats (4×10^5 cells) with irradiated (30 Gy) RPMI-8866 cells (10^5 cells) at 37°C for 10 to 13 days, as previously described (33).

Cytotoxicity and degranulation assay

NK cell cytotoxic activity and degranulation assay were performed by a standard 4-hour ^{51}Cr-release assay and flow cytometric analysis of cell-surface CD107a expression, respectively, as previously described (30). Specific lysis was converted to lytic units (L.U.) calculated from the curve of the percentage lysis (34). One lytic unit was defined as the number of NK cells required to produce 20% lysis of 10^6 target cells during the 4 hours of incubation.

Statistical analysis

Statistical significance was assessed by the two-tailed paired Student *t* test. Raw assay data were normalized as the fraction (percentage) of the highest values obtained for each assay. Normalized values were analyzed for correlation by the regression analysis using GraphPad software. *P* values not exceeding 0.05 were considered to be statistically significant.

Results

ERAP1 suppression by RNAi in human tumor cell lines

First, we tested four shRNA constructs targeting different regions of ERAP1 (abbreviated to shERAP1) in HeLa cells. The shERAP1 #42 construct that provided the highest RNAi efficiency and specificity, as determined by qPCR and Western blotting (Supplementary Fig. S1), was selected and used in five human tumor cell lines: Raji, SK-N-SH, SK-MEL-93, MNT-1, and DAOY (Fig. 1A; Supplementary Table S1). Compared with control shRNA-transduced cells (abbreviated to shCTRL), ERAP1 expression was suppressed almost completely in four shERAP1-transduced tumor cells, Raji, SK-N-SH, SK-MEL-93, and DAOY, the only exception being represented by MNT-1, which showed a moderate suppression, as evaluated at protein level (Fig. 1A). On the other hand, MHC-I surface expression moderately decreased in MNT-1–shERAP1 and DAOY-shERAP1 cells, whereas it increased in HeLa-shERAP1 cells, as compared with the relative controls (Fig. 1B). No change in MHC-I expression was detectable in the other shERAP1 tumor cells, Raji, SK-N-SH, and SK-MEL-93.

NK cell stimulation with shERAP1-transduced human tumor cell lines

The shERAP1 tumor cells were then assayed for the ability of inducing NK cell degranulation. Freshly isolated NK cells were cocultured with shERAP1 tumor cells at different ratios and CD107a expression on NK cell subset was determined by flow cytometric analysis. As expected, CD107a expression was

Published OnlineFirst January 15, 2015; DOI: 10.1158/0008-5472.CAN-14-1643

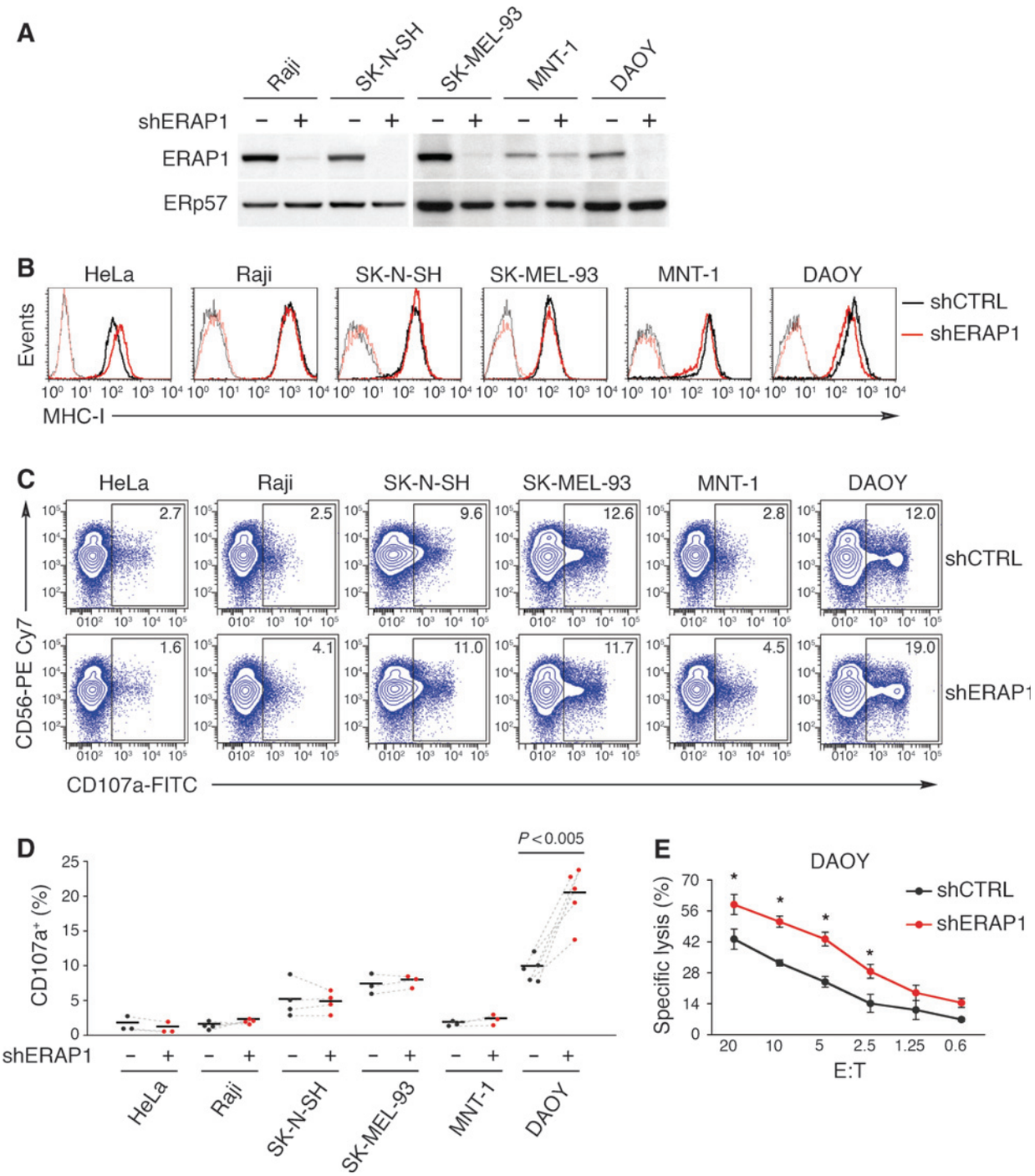

Figure 1.
Inhibition of ERAP1 expression activates NK cell recognition in response to DAOY cells. A, immunoblotting analysis of ERAP1 expression in tumor cell lines transduced with lentiviral vectors encoding either control shRNA (shCTRL, −) or ERAP1 shRNA (shERAP1, +). An ERp57 Ab was used for normalization. B, flow cytometric analysis of surface MHC-I expression in tumor cell lines of A using mAb W6/32 (bold lines). Isotype-matched negative control antibodies are displayed as dotted lines. C, representative example of degranulation by human $CD3^{-}CD56^{+}$ NK cells from a healthy donor, measured as CD107a cell-surface expression following stimulation with the indicated target cells. The percentage of $CD107a^{+}$ NK cells is indicated. D, summary of NK cell degranulation after stimulation with shCTRL or shERAP1 tumor cells (black and red dots, respectively). Horizontal bars represent the average values of $CD107a^{+}$ NK cell subsets. Dots, number of donor cells tested. Dashed lines connect data obtained from each donor with the indicated targets. E, DAOY-shERAP1 and DAOY-shCTRL cells were assayed as targets of NK cells at the indicated effector:target (E:T) ratios in a standard ^{51}Cr-release assay. A representative of five independent experiments is reported. *P* values, compared with DAOY-shERAP1 and DAOY-shCTRL cells (two-tailed paired Student *t* test); *, $P < 0.001$.

Published OnlineFirst January 15, 2015; DOI: 10.1158/0008-5472.CAN-14-1643

upregulated on NK cells following stimulation with the MHC-I–negative K562 target cell line (Supplementary Fig. S2). As shown in Fig. 1C, CD107a expression was significantly upregulated by stimulation with DAOY-shERAP1 cells as compared with DAOY-shCTRL cells. The mean frequency of $CD107a^+$ cells in 5 different donors was 21.6 ± 3.4 for DAOY-shERAP1 and 9.8 ± 1.7 for DAOY-shCTRL (Fig. 1D). In spite of impaired MHC-I expression, MNT-1–shERAP1 cells were not stimulatory. No significant stimulation was also observed for HeLa-shERAP1, Raji-shERAP1, SK-N-SH–shERAP1, and SK-MEL-93–shERAP1 cells as compared with their relative controls (Fig. 1C and D).

The NK cell degranulation seen in response to DAOY-shERAP1 was also significantly associated with enhanced NK cell killing as evaluated by ^{51}Cr release assay (Fig. 1E). Conversely, phosphorylation of the SHP-1 substrate Vav-1, a signaling mediator of the NK cell–activation state, appeared not to be affected by ERAP1 inhibition (not shown). This could depend on the use of polyclonal NK cells with a great array of inhibitory and activating pathways involved in the interaction with MHC-I–expressing DAOY cells, instead of NK cell models overexpressing single KIRs (35).

Thus among six human tumor cell lines, only DAOY-shERAP1 induces a fully functional activation of NK cells.

Two mechanisms may explain NK cell activation in response to DAOY-shERAP1. First, ERAP1 inhibition may cause an increased expression of ligands for activating NK cell receptors on DAOY cells. Second, ERAP1 inhibition may result in a conformational change of pMHC-I complexes, which impairs the engagement of inhibitory receptors. As shown in Fig. 2A, ERAP1 inhibition did not affect the expression of the known ligands for NK cell–activating receptors in DAOY cells, except for a slight downregulation of ULBP3.

Then, we evaluated the ability of NK cells to kill DAOY-shERAP1 after the replacement of endogenous MHC-I peptides with a large excess of the high-affinity HLA class I–restricted I9W, T9I, and E9Y peptides (Supplementary Table S2). Although these peptides did not change MHC-I surface expression (Supplementary Fig. S3), they totally inhibited DAOY-shERAP1-induced NK cell degranulation (Fig. 2B and C). In contrast, the irrelevant S8L peptide neither changed MHC-I expression nor induced NK cell degranulation. The mean frequencies of $CD107a^+$ cells obtained from 5 donors for unpulsed, I9W/T9I/E9Y-pulsed, and S8L-pulsed DAOY-shERAP1 were 20.74 ± 1.7, 12.26 ± 1.4, and 21.38 ± 1.9, respectively (Fig. 2C).

Therefore, NK cells kill DAOY-shERAP1 cells because of the impaired engagement of pMHC-I complexes with inhibitory NK cell receptors.

Analysis of NK cell responses to DAOY-shERAP1 cells

To evaluate whether inhibitory receptors are involved in NK cell activation in response to DAOY-shERAP1, we used three different approaches: (i) to evaluate the binding of KIR fusion proteins to DAOY-shCTRL and DAOY-shERAP1 cells, (ii) to investigate the aggregation of KIRs at the interface between NK cells and DAOY target cells (24, 35, 36), (iii) to analyze CD107a expression in distinct NK cell subsets. We focused on three inhibitory receptors, KIR2DL1, KIR2DL3, and KIR3DL1, whose ligands are expressed in DAOY cells (Supplementary Table S1), and for which MHC-I engagements have been shown to depend on the repertoire of pMHC-I complexes (20, 21, 23, 25, 36).

In the first approach, DAOY cells were stained with KIR–Fc fusion proteins KIR2DL1–Fc, KIR2DL3–Fc, and KIR3DL1–Fc and analyzed by flow cytometry. As compared with control cells, ERAP1 inhibition caused a significant reduction in the binding of KIR2DL3–Fc and KIR3DL1–Fc (0.56 ± 0.04 and 0.65 ± 0.08, respectively). No binding was seen for KIR2DL1–Fc (Fig. 3A and B).

In the second and last approach, NK cells from individuals coexpressing all three inhibitory KIRs with their KIR ligands and devoid of activating KIRs, with the exception of KIR2DS4 (A/A genotype; Supplementary Tables S3 and S4), were isolated and incubated with DAOY-shERAP1 and DAOY-shCTRL cells. Conjugates were stained for KIR2DL3 and analyzed by confocal microscopy. Images of the contact area showed that DAOY-shERAP1 and DAOY-shCTRL cells induced the formation of differently structured synapses (Fig. 3C). Silencing of ERAP1 resulted in a more diffuse clustering of KIR2DL3, as compared with control cells. The level of KIR2DL3 accumulation at the contact area between NK and DAOY-shERAP1 cells was significantly lower than that measured between NK and DAOY-shCTRL cells (1.50 ± 0.04 vs. 1.10 ± 0.03-fold, respectively; Fig. 3D). Furthermore, the percentage of total conjugates with tight clustering of KIR2DL3 at the synapse area (fold increase>1.5) was lower with DAOY-shERAP1 cells than with DAOY-shCTRL cells (10 ± 1.5 vs. 55 ± 6, respectively; Fig. 3E). Thus, consistently with enhanced NK cell killing, the accumulation of KIR2DL3 recruited to the immune synapse was reduced in response to DAOY-shERAP1 as compared with DAOY-shCTRL.

In the last approach, NK cells cocultured with DAOY-shERAP1 cells or DAOY-shCTRL cells were stained with a panel of specific antibodies and analyzed by flow cytometry. The gating strategy used to evaluate the contribution of single inhibitory receptors is shown in Supplementary Fig. S4. NK cell subsets expressing the single inhibitory KIRs [KIR2DL3 single positive (KIR2DL3sp), KIR2DL1sp, KIR3DL1sp], CD94-NKG2Asp– or CD94-NKG2A–negative and KIR-triple negatives (NKG2An and KIRtn) were all responsive to stimulation with DAOY-shCTRL cells (Fig. 4A and B). CD107a expression in NK cell subsets significantly increased up to 2.3-fold when stimulated with DAOY-shERAP1 cells. The average percentages of $CD107a^+$ cells for DAOY-shCTRL versus DAOY-shERAP1 were 11.12 ± 1.7 versus 24.77 ± 1.9 for KIR2DL3sp subset, 10.02 ± 0.7 versus 22.60 ± 1.4 for KIR2DL1sp subset, and 7.95 ± 0.6 versus 18.70 ± 1.6 for KIR3DL1sp subset (Fig. 4B). A significant difference was found also for a CD94-NKG2Asp subset (7.87 ± 0.9 vs. 16.82 ± 1.5, respectively; Fig. 4B).

Thus, ERAP1 inhibition results in increased NK cell–mediated killing due to an impaired engagement of both inhibitory KIRs and CD94-NKG2A receptor.

NK cell recognition of DAOY cells treated with leucinethiol

To investigate the effect of pharmacological inhibition of ERAP1 on NK cell killing, DAOY cells were treated with leucinethiol (Leu-SH), a potent inhibitor of aminopeptidases, including ERAP1 (37), and then evaluated for their ability to induce NK cell degranulation.

Treatment with Leu-SH decreased ERAP1 activity of DAOY cells by 94% and MHC-I surface expression by 30% (Fig. 5A and B) as compared with control dithiothreitol (DTT)-treated cells, this inhibition being similar to that observed using shERAP1. Leu-SH treatment significantly enhanced degranulation, that is, CD107a expression of NK cells (Fig. 5C). The average percentage

Published OnlineFirst January 15, 2015; DOI: 10.1158/0008-5472.CAN-14-1643

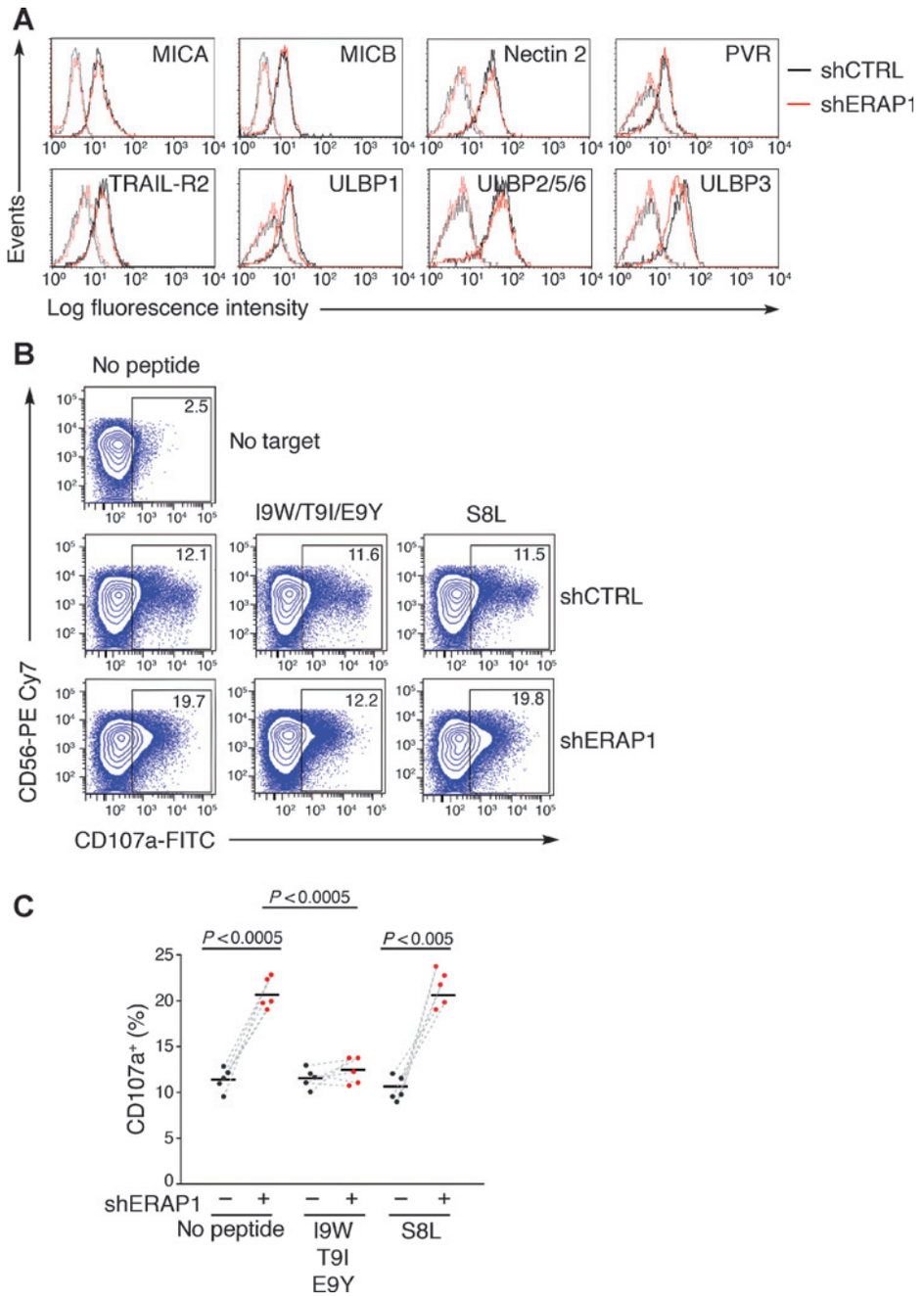

Figure 2.
Peptide-specific protection of DAOY-shERAP1 cells against NK cell–mediated degranulation. A, flow cytometric analysis of the indicated ligands for activating NK cell receptors on DAOY-shCTRL and DAOY-shERAP1 cells (black and red lines, respectively). Isotype-matched negative control antibodies are displayed as dotted lines. B, representative example of degranulation by human $CD3^{-}CD56^{+}$ NK cells from a healthy donor, measured as CD107a cell-surface expression following stimulation with target cells pretreated with low pH buffer to allow dissociation of preformed pMHC class I complexes and then pulsed or not (no peptide) with the indicated peptides. The percentage of $CD107a^{+}$ NK cells is indicated. A representative of five independent experiments is reported. C, summary of NK cell degranulation after stimulation with pretreated DAOY-shCTRL or DAOY-shERAP1 cells (black and red dots, respectively) is shown as in Fig. 1D. *P* values, compared with DAOY-shERAP1 and DAOY-shCTRL cells (two-tailed paired Student *t* test).

of $CD107a^{+}$ NK cells of 9 donors was 3.32 ± 2.6 for DTT treatment and 14.12 ± 2.9 for Leu-SH treatment (Fig. 5D). It is noteworthy that Leu-SH treatment did not affect the expression of activating ligands in DAOY cells (Supplementary Fig. S5), but caused a significant reduction in the binding of KIR2DL3–Fc and KIR3DL1–Fc (Supplementary Fig. S6A), similarly to what observed for DAOY-shERAP1 cells.

CD107a expression in NK cell subsets significantly increased up to 2.9-fold when stimulated with Leu-SH–treated DAOY cells (Supplementary Figs. S6B and S5E). Average percentages of $CD107a^{+}$ cells obtained from 4 donors of DTT-treated versus Leu-SH–treated cells were 12.42 ± 1.6 versus 27.90 ± 3.6 for KIR2DL3sp subset, 9.27 ± 1.4 versus 25.60 ± 3.0 for KIR2DL1sp subset, 7.42 ± 1.0 versus 15.47 ± 1.1 for KIR3DL1sp subset, and 12.32 ± 0.9 versus 22.7 ± 2.1 for a CD94-NKG2Asp subset (Fig. 5E).

These results indicate that Leu-SH may function as a potent activator of NK cell immune response against cancer.

Leu-SH treatment affects NK cell recognition of autologous LCLs

To evaluate the potential effectiveness of ERAP1 inhibition for clinical applications, LCLs generated from 20 healthy donors were

Published OnlineFirst January 15, 2015; DOI: 10.1158/0008-5472.CAN-14-1643

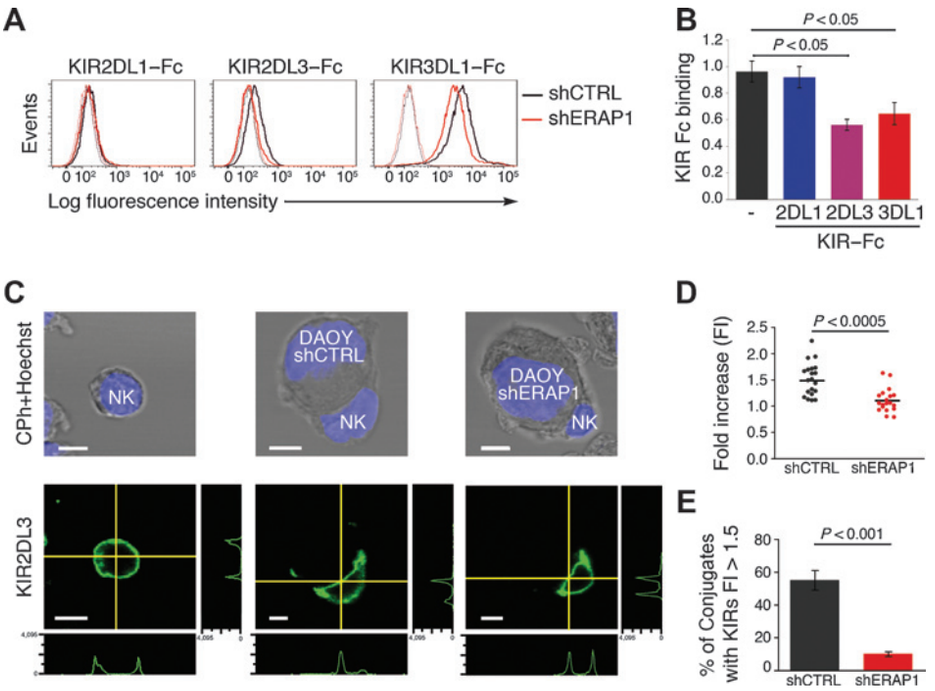

Figure 3.
Inhibition of ERAP1 decreases KIR binding to DAOY cells and KIR aggregation at the interface between NK and target cells. A, flow cytometric analysis of KIR–Fc fusion protein binding to DAOY-shCTRL and DAOY-shERAP1 cells (black and red lines, respectively). Isotype-matched negative control antibodies are displayed as dotted lines. B, the relative intensity in KIR–Fc binding to MHC-I molecules on DAOY-shERAP1 compared with DAOY-shCTRL cells. Means ± SD of three independent experiments are shown. C, clustering at the interface between NK cells and DAOY-shCTRL or DAOY-shERAP1 cells. NK and target cells were coincubated 10 minutes at 37°C. The formed conjugates were fixed and stained with anti-KIR2DL3 (mAb GL-183). Representative example of confocal microscopy images of NK cells alone and conjugates between NK and DAOY-shCTRL or DAOY-shERAP1 cells. Phase contrast and nuclear staining (by Hoechst) were used to distinguish effector by target cells. Fluorescence intensity and plot profile on a scale from 0 to 4095 of mean fluorescence intensity, resulting from the intersection of vertical and horizontal axes of both contact and noncontact area on NK cell membrane observed in the central plane, were reported to evaluate inhibitory KIR accumulation in synapse area in respect to noncontact area. D, the fold increase in fluorescence intensity at the immune synapse area was calculated as a ratio of the mean fluorescence intensity of the entire conjugation area compared with the mean fluorescence intensity along the rest of the NK cell membrane for each conjugation. These values were both corrected for background fluorescence, as measured within an empty region of the image. Horizontal bars, average values. E, the percentage of conjugates showing a KIR2DL3 aggregation with a fold increase ≥1.5 at the interface between NK cells and target cells was depicted as the mean for cells from three donors tested in three independent experiments. D and E, a minimum of 20 conjugates was counted for each condition per experiment. *P* values were obtained by the two-tailed paired Student *t* test.

treated with Leu-SH. These cells were then evaluated for MHC-I surface expression and tested as target for NK cells isolated from the same subjects, that is, in the autologous setting.

MHC-I surface expression decreased by up to 50% in samples 1 to 7, whereas it increased by up to 60% in samples 12 to 20; samples 8 to 11 showed minor changes not exceeding 10% (Fig. 6A; Supplementary Table S5). Interestingly, HLA class I typing revealed that samples 1 to 7 were enriched for HLA-B7 supertype alleles (38) and/or for HLA-C alleles C*06:02 and C*07:02 (39, 40), compared with the other samples (Supplementary Table S5 and Supplementary Fig. S7). This finding may be relevant to the enzymatic specificity of ERAP1 and suggests that ERAP1 activity enhanced the generation of peptides that bind to these HLA class I alleles.

Next, NK cells obtained from the same donors were tested for their ability to kill Leu-SH–treated LCLs. As shown for each of the 18 LCLs tested, the mean value of NK cell killing was significantly higher for 11 Leu-SH–treated LCLs, which had reduced or unchanged MHC-I surface expression, compared with the control DTT-treated LCLs (Fig. 6B; Supplementary Table S5). The mean of L.U. 20% was 5.36 versus 10.54 for DTT- versus Leu-SH–treated LCLs. Such differences were not seen for the 7 Leu-SH–treated LCLs that had enhanced MHC-I expression. The mean of L.U. 20% was 3.86 versus 3.63 for DTT- versus Leu-SH–treated LCLs. In the regression analysis of the whole dataset, including LCLs with enhanced, unchanged, and decreased MHC-I expression, the correlation between surface MHC-I and L.U. 20%, both evaluated as fold change of Leu-SH–treated/DTT–treated LCLs, was significant with an R^2 value of 0.23 ($P < 0.05$; Fig. 6C).

Altogether, these data indicate that: (i) Leu-SH treatment either downregulates or enhances MHC-I expression in LCLs; (ii) MHC-I downregulation occurs more frequently in cells with HLA-B alleles belonging to HLA-B7 supertype and/or HLA-C alleles C*04:01, C*06:02 and C*07:02; and (iii) LCLs with reduced MHC-I expression are more susceptible to NK cell killing.

Leu-SH treatment affects NK cell recognition of allogeneic LCLs

Next, NK cells were tested for their ability to kill Leu-SH–treated LCLs in an allogeneic setting. NK cell alloreactivity is expected to take place when the inhibitory KIRs expressed on NK cells are not engaged by the HLA class I ligands expressed on the target cells because the inhibitory signal is not generated. On the basis of this

Published OnlineFirst January 15, 2015; DOI: 10.1158/0008-5472.CAN-14-1643

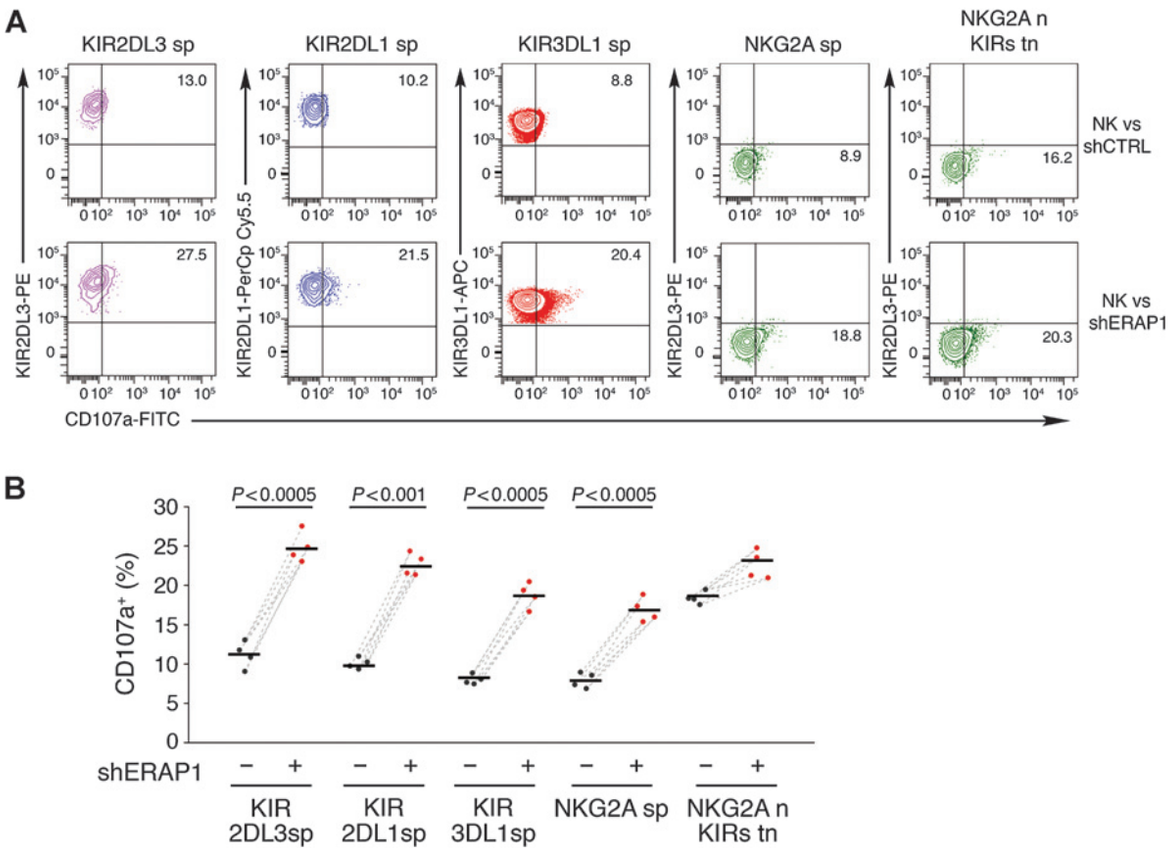

Figure 4.
Inhibition of ERAP1 enhanced NK cell killing of DAOY cells by affecting the engagement of KIRs. A, representative example of degranulation by human $CD3^-CD56^+$ NK cells from the donor D (see Supplementary Table S3) coexpressing KIR2DL1, KIR2DL3, and KIR3DL1 and devoid of activating KIRs, measured as CD107a cell-surface expression in response to DAOY-shERAP1 and DAOY-shCTRL cells. The color code used to define the NK cell subsets positive for single KIRs (KIR sp) or NKG2A (NKG2A sp) or negative (n) for NKG2A and triple negative (tn) for KIRs (NKG2A n and KIR tn) are shown in Supplementary Fig. S4. The percentage of $CD107a^+$ cells within the indicated NK cell subsets is shown. B, summary of NK cell degranulation of cells from four donors after stimulation with DAOY-shERAP1 or DAOY-shCTRL (red and black dots, respectively) is shown as in Fig. 1D. *P* values, compared with DAOY-shERAP1 and DAOY-shCTRL cells (two-tailed paired Student *t* test).

assumption, NK cells isolated from 15 donors were tested against allogeneic LCLs at various combinations. The KIR gene profile of the donors is shown in Supplementary Table S6. As shown in Fig. 7 and Supplementary Table S7, the two groups of effector/target pairs with alloreactive and nonalloreactive NK cells consist of 11 pairs. Assay data were presented separately for these two groups as the percentage of L.U. 20% of Leu-SH–treated/DTT–treated LCLs. Regardless of the presence or absence of alloreactive NK cells, remarkably variable levels of NK cell killing were found in both groups (Fig. 7A; Supplementary Table S7).

Data were also shown as L.U. 20% relatively to either decreased or increased MHC-I expression (Fig. 7B). NK cell cytotoxicity was significantly enhanced in Leu-SH–treated LCLs, which showed decreased MHC-I expression, as compared with the DTT-treated LCLs ($P < 0.005$). Such difference was not statistically significant for Leu-SH–treated LCLs, which showed increased MHC-I expression, as compared with the DTT-treated LCLs (Fig. 6B).

Altogether, these data indicate that Leu-SH treatment enhances the susceptibility of LCLs to NK cell killing also in the allogeneic settings regardless of the involved KIR–KIR ligand matching.

Discussion

We demonstrate that the loss of ERAP1 function in human cell lines enhances their susceptibility to NK cell killing by perturbing recognition of pMHC-I complexes by inhibitory KIRs and CD94-NKG2A receptor. This depends on the pMHC-I repertoire, because replacement of endogenous peptides with known high-affinity peptides is sufficient to revert the susceptibility of DAOY-shERAP1 cells to NK cell killing. To our knowledge, this is the first demonstration that ERAP1 plays a key role in generating functional ligands for human NK cell inhibitory receptors, and that its inhibition can be useful for improving NK cell–based cancer immunotherapy.

ERAP1 has been found to have a dual function in antigen processing, being able to generate (27, 41), but also completely destroy MHC-I–bound peptides (42, 43). ERAP1 inhibition is expected to increase or decrease the presentation of epitopes normally destroyed or generated by the enzyme. Consistent with this dual role, we found that ERAP1 inhibition differently affects MHC-I surface expression in human cell lines, being decreased, increased, or unchanged. It is possible that MHC-I alleles displaying unchanged surface expression levels could be

Published OnlineFirst January 15, 2015; DOI: 10.1158/0008-5472.CAN-14-1643

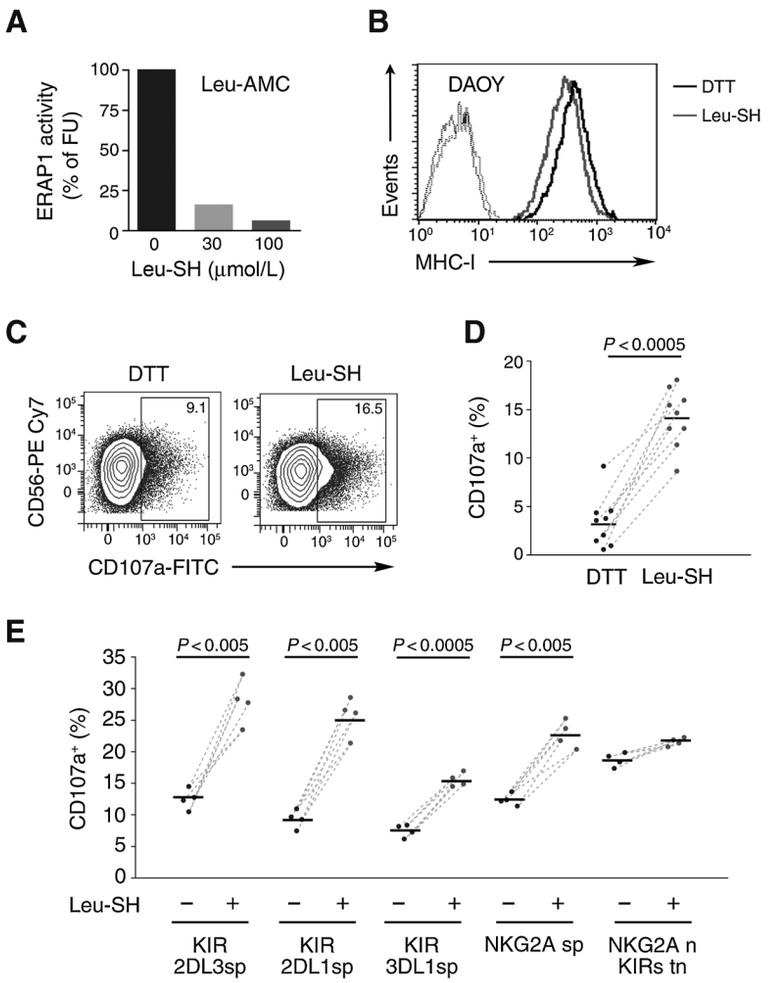

Figure 5.
Leu-SH treatment affects NK cell recognition of DAOY cells. A, ERAP1 activity was detected in DAOY cells pretreated 18 hours at 37°C with either 0.5 mmol/L DTT (0) or 30 μmol/L Leu-SH (30) or 100 μmol/L Leu-SH (100). Data are reported in fluorescence units. B, flow cytometric analysis of surface MHC-I expression in DTT- or Leu-SH–treated (100 μmol/L) DAOY cells using mAb W6/32 (bold lines). Isotype-matched negative controls are displayed as thin lines. C, flow cytometric analysis of CD107a expression in $CD3^-CD56^+$ NK cells cocultured with either DTT- or Leu-SH–treated DAOY cells. The percentage of $CD107a^+$ NK cells is indicated. D, summary of NK cell degranulation of cells from nine donors after stimulation with DTT- or Leu-SH–treated DAOY cell lines is shown as in Fig. 1D. E, summary of NK cell degranulation measured as CD107a cell-surface expression of cells from four donors is shown as above *P* values, compared with DTT- and Leu-SH treatments (two-tailed paired Student *t* test).

insensitive to ERAP1 knockdown. In general, cells with decreased MHC-I levels were more susceptible to NK cell killing, as seen for DAOY and for LCLs tested with either autologous or allogeneic NK cells. Of note, these cells express HLA-class I alleles that bind preferentially peptides with a proline residue in position 2 (38–40). These peptides have very low affinity for the transporter associated with antigen processing (TAP; ref. 44), and enter into ER as NH_2 terminal–extended precursors that are trimmed before assembly with MHC-I molecules (26, 29, 37). The MHC-I consensus motif with a proline at position 2 accounts for mouse L^d and more than 33% and 36% of all known human HLA-B and HLA-C motifs in the Italian population (45). Thus, one third of individuals carrying these HLA class I alleles will react with reduced surface expression upon ERAP1 inhibition.

In the absence of ERAP1, precursor peptides form unstable pMHC-I complexes, which are not sufficiently conformed to assure the interaction with NK cell inhibitory receptors, or T-cell receptors (30, 41). Indeed, we have shown that NK cell activation is not due to a simple quantitative reduction in surface MHC-I expression, as pulsing with high-affinity trimmed peptides rescued the inhibitory activity of NK cells.

Altogether our findings suggest that pharmacologic inhibition of ERAP1 activity may have important therapeutic applications in cancer immunotherapy, being as efficient as the genetic downregulation of ERAP1 to induce NK cell–mediated immunity. In addition to the inhibitor Leu-SH, which has been successfully used to reproduce the effects of genetic ERAP1 suppression (30, 46), a novel class of more potent ERAP1 inhibitors has been recently described (43). These new compounds are effective in targeting *in vitro* ERAP1 inside the ER at the nmol/L level, and modulate cytotoxic T lymphocyte responses, suggesting their potential use for the pharmacologic manipulation of both NK cell and T-cell antitumor activity.

NK cell–based adoptive immunotherapy represents a fascinating approach for adjuvant treatment of many cancers. One of the most promising settings to test the adoptive infusion of allogeneic NK cells is hematopoietic stem cell transplantation (HSCT; ref. 47). In patients with leukemia undergoing haploidentical HSCT, the use of donors with alloreactive NK cells displaying antileukemia activity is associated with a lower risk of leukemia recurrence without increasing the risk of graft-versus-host disease (48). The success of this approach is explained by the transplantation of donor-derived alloreactive NK cells, which persist in patients after haploidentical HSCT for years, contributing to the eradication of malignant cells (32).

Currently, a wide variety of new drugs able to strengthen NK cell response are being tested in clinical trials (49), but a toxic effect

Published OnlineFirst January 15, 2015; DOI: 10.1158/0008-5472.CAN-14-1643

has been reported for some of them (50). Here, we demonstrated that inhibition of ERAP1 renders LCLs more susceptible to killing by autologous and allogeneic NK cells, causing NK cell alloreactivity also in donor-recipient pairs where it is not expected because of KIR–KIR ligand matching. Development of small molecules targeting ERAP1 might provide an innovative tool to improve outcome of NK cell–based antitumor therapy protocols.

In summary, we have demonstrated that either pharmacologic or genetic inhibition of ERAP1 function could represent a novel tool for overcoming classical and nonclassical MHC-I–mediated inhibition of NK cell killing, leading to a more successful cancer immunotherapy.

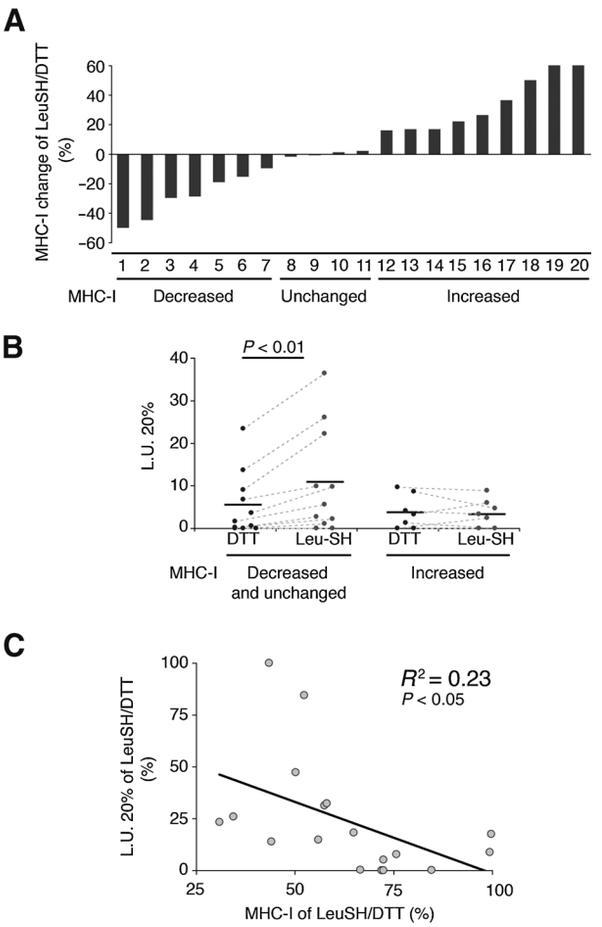

Figure 6.
Leu-SH treatment affects NK cell recognition of autologous LCLs. A, flow cytometric analysis of surface MHC-I expression in LCLs treated with either 0.5 mmol/L DTT or 100 μmol/L Leu-SH for 18 hours at 37°C and stained with mAb W6/32. Data are presented as indicated in Materials and Methods. B, NK cells were tested as effectors in a standard ^{51}Cr-release assay on the autologous DTT- and Leu-SH–treated LCLs. Specific lysis was converted to L.U. 20%. Effector/target pairs were clustered in two groups based on MHC-I change following Leu-SH treatment. Dots, L.U. 20% of the effector/target pairs tested; horizontal bars, average values. Dashed lines connect L.U. 20% from each donor cell obtained with the indicated target. C, regression analysis of mean fluorescence intensity and L.U. 20% fold changes of Leu-SH–treated and DTT-treated cells, both expressed as the percentage of the highest value obtained for each assays and plotted against each other (see Materials and Methods). Regression line and coefficient are shown. *P* value, compared with DTT- and Leu-SH treatments (two-tailed paired Student *t* test).

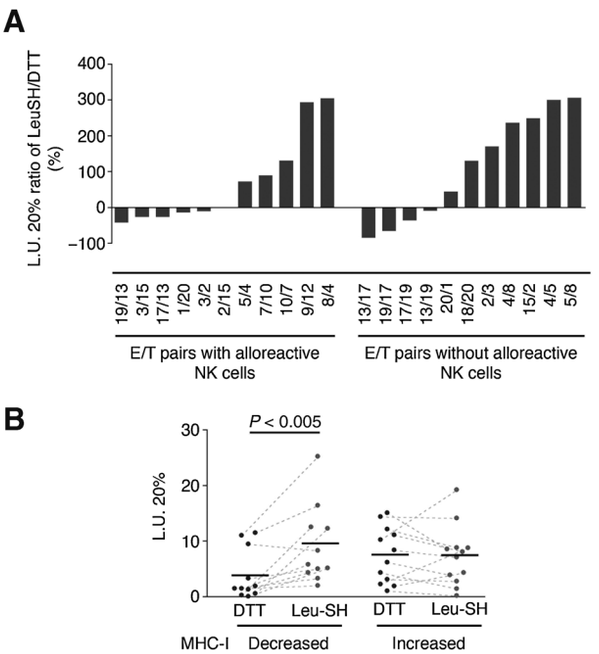

Figure 7.
Leu-SH treatment affects NK cell recognition of allogeneic LCLs. NK cells were tested as effectors in a standard ^{51}Cr-release assay with allogeneic DTT- and Leu-SH–treated LCLs. A, specific lysis was converted to L.U. 20% and presented as ratio between Leu-SH–treated cells and DTT-treated cells by clustering effector/target (E/T) pairs in two groups based on the presence or absence of alloreactive NK cells. B, L.U. 20% of DTT- and Leu-SH–treated LCLs were displayed by clustering E/T pairs in two groups based on MHC-I fold change as in Fig. 6A. Horizontal bars, average L.U. 20% values. Dashed lines connect L.U. 20% from each donor cell obtained with the indicated targets. *P* value, compared with DTT- and Leu-SH treatments (two-tailed paired Student *t* test).

Disclosure of Potential Conflicts of Interest

No potential conflicts of interest were disclosed.

Disclaimer

The funders had no role in study design, data collection and analysis, decision to publish, or preparation of the article.

Authors' Contributions

Conception and design: L. Cifaldi, P. Romania, F. Locatelli, D. Fruci
Development of methodology: L. Cifaldi, P. Romania, R. Meazza, D. Pende, D. Fruci
Acquisition of data (provided animals, acquired and managed patients, provided facilities, etc.): L. Cifaldi, M. Falco, S. Lorenzi, S. Petrini, D. Fruci
Analysis and interpretation of data (e.g., statistical analysis, biostatistics, computational analysis): L. Cifaldi, P. Romania, R. Meazza, D. Pende, D. Fruci
Writing, review, and/or revision of the manuscript: L. Cifaldi, P. Romania, M. Falco, R. Meazza, M. Andreani, D. Pende, F. Locatelli, D. Fruci
Administrative, technical, or material support (i.e., reporting or organizing data, constructing databases): L. Cifaldi, D. Pende, D. Fruci
Study supervision: L. Cifaldi, D. Pende, F. Locatelli, D. Fruci
Other (tissue typing): M. Andreani

Acknowledgments

The authors thank L. Moretta, A. Santoni, P. van Endert, R. Molfetta, and R. Carsetti for providing reagents and critical reading of the article.

Grant Support

This work was supported by Italian Ministry of Health (Rome, Italy) grants PE-2011-02351866 (D. Fruci), RF-2010-2316606 (F. Locatelli and D. Pende), RF-2010-2316319 (D. Pende), and the Special Project "5 × 1,000" Associazione Italiana per la Ricerca sul Cancro (AIRC, Milan, Italy) grant #9962 (F. Locatelli).

The costs of publication of this article were defrayed in part by the payment of page charges. This article must therefore be hereby marked *advertisement* in accordance with 18 U.S.C. Section 1734 solely to indicate this fact.

Received June 4, 2014; revised December 19, 2014; accepted December 22, 2014; published OnlineFirst January 15, 2015.

References

1. Lanier LL. NK cell recognition. Annu Rev Immunol 2005;23:225–74.
2. Raulet DH, Vance RE. Self-tolerance of natural killer cells. Nat Rev Immunol 2006;6:520–31.
3. Raulet DH, Vance RE, McMahon CW. Regulation of the natural killer cell receptor repertoire. Annu Rev Immunol 2001;19:291–330.
4. Lanier LL. Evolutionary struggles between NK cells and viruses. Nat Rev Immunol 2008;8:259–68.
5. Orr MT, Murphy WJ, Lanier LL. `Unlicensed' natural killer cells dominate the response to cytomegalovirus infection. Nat Immunol 2010;11:321–7.
6. Cerwenka A, Lanier LL. Natural killer cells, viruses, and cancer. Nat Rev Immunol 2001;1:41–9.
7. Diefenbach A, Jensen ER, Jamieson AM, Raulet DH. Rae1 and H60 ligands of the NKG2D receptor stimulate tumour immunity. Nature 2001;413:165–71.
8. Colonna M, Samaridis J. Cloning of immunoglobulin-superfamily members associated with HLA-C and HLA-B recognition by human natural killer cells. Science 1995;268:405–8.
9. Moretta A, Bottino C, Vitale M, Pende D, Biassoni R, Mingari MC, et al. Receptors for HLA class-I molecules in human natural killer cells. Annu Rev Immunol 1996;14:619–48.
10. Braud VM, Allan DS, O'Callaghan CA, Soderstrom K, D'Andrea A, Ogg GS, et al. HLA-E binds to natural killer cell receptors CD94/NKG2A, B and C. Nature 1998;391:795–9.
11. Karlhofer FM, Ribaudo RK, Yokoyama WM. MHC class I alloantigen specificity of Ly-49$^+$ IL-2-activated natural killer cells. Nature 1992;358:66–70.
12. Kim S, Sunwoo JB, Yang L, Choi T, Song YJ, French AR, et al. HLA alleles determine differences in human natural killer cell responsiveness and potency. Proc Natl Acad Sci U S A 2008;105:3053–8.
13. Anfossi N, Andre P, Guia S, Falk CS, Roetynck S, Stewart CA, et al. Human NK cell education by inhibitory receptors for MHC class I. Immunity 2006;25:331–42.
14. Joncker NT, Fernandez NC, Treiner E, Vivier E, Raulet DH. NK cell responsiveness is tuned commensurate with the number of inhibitory receptors for self-MHC class I: the rheostat model. J Immunol 2009;182:4572–80.
15. Hoglund P, Brodin P. Current perspectives of natural killer cell education by MHC class I molecules. Nat Rev 2010;10:724–34.
16. Kim S, Poursine-Laurent J, Truscott SM, Lybarger L, Song YJ, Yang L, et al. Licensing of natural killer cells by host major histocompatibility complex class I molecules. Nature 2005;436:709–13.
17. Vilches C, Parham P. KIR: diverse, rapidly evolving receptors of innate and adaptive immunity. Annu Rev Immunol 2002;20:217–51.
18. Colonna M, Borsellino G, Falco M, Ferrara GB, Strominger JL. HLA-C is the inhibitory ligand that determines dominant resistance to lysis by NK1- and NK2-specific natural killer cells. Proc Natl Acad Sci U S A 1993;90:12000–4.
19. Wagtmann N, Rajagopalan S, Winter CC, Peruzzi M, Long EO. Killer cell inhibitory receptors specific for HLA-C and HLA-B identified by direct binding and by functional transfer. Immunity 1995;3:801–9.
20. Boyington JC, Motyka SA, Schuck P, Brooks AG, Sun PD. Crystal structure of an NK cell immunoglobulin-like receptor in complex with its class I MHC ligand. Nature 2000;405:537–43.
21. Fan QR, Long EO, Wiley DC. Crystal structure of the human natural killer cell inhibitory receptor KIR2DL1-HLA-Cw4 complex. Nat Immunol 2001;2:452–60.
22. Hoare HL, Sullivan LC, Clements CS, Ely LK, Beddoe T, Henderson KN, et al. Subtle changes in peptide conformation profoundly affect recognition of the nonclassical MHC class I molecule HLA-E by the CD94–NKG2 natural killer cell receptors. J Mol Biol 2008;377:1297–303.
23. Stewart CA, Laugier-Anfossi F, Vely F, Saulquin X, Riedmuller J, Tisserant A, et al. Recognition of peptide-MHC class I complexes by activating killer immunoglobulin-like receptors. Proc Natl Acad Sci U S A 2005;102:13224–9.
24. Cheent KS, Jamil KM, Cassidy S, Liu M, Mbiribindi B, Mulder A, et al. Synergistic inhibition of natural killer cells by the nonsignaling molecule CD94. Proc Natl Acad Sci U S A 2013;110:16981–6.
25. Cassidy SA, Cheent KS, Khakoo SI. Effects of Peptide on NK cell–mediated MHC I recognition. Front Immunol 2014;5:133.
26. Serwold T, Gonzalez F, Kim J, Jacob R, Shastri N. ERAAP customizes peptides for MHC class I molecules in the endoplasmic reticulum. Nature 2002;419:480–3.
27. Saric T, Chang SC, Hattori A, York IA, Markant S, Rock KL, et al. An IFN-gamma-induced aminopeptidase in the ER, ERAP1, trims precursors to MHC class I-presented peptides. Nat Immunol 2002;3:1169–76.
28. York IA, Chang SC, Saric T, Keys JA, Favreau JM, Goldberg AL, et al. The ER aminopeptidase ERAP1 enhances or limits antigen presentation by trimming epitopes to 8–9 residues. Nat Immunol 2002;3:1177–84.
29. Saveanu L, Carroll O, Lindo V, Del Val M, Lopez D, Lepelletier Y, et al. Concerted peptide trimming by human ERAP1 and ERAP2 aminopeptidase complexes in the endoplasmic reticulum. Nat Immunol 2005;6:689–97.
30. Cifaldi L, Lo Monaco E, Forloni M, Giorda E, Lorenzi S, Petrini S, et al. Natural killer cells efficiently reject lymphoma silenced for the endoplasmic reticulum aminopeptidase associated with antigen processing. Cancer Res 2011;71:1597–606.
31. Chersi A, Galati R, Accapezzato D, Francavilla V, Barnaba V, Butler RH, et al. Responses of peptide-specific T cells to stimulation with polystyrene beads carrying HLA class I molecules loaded with single peptides. J Immunol Methods 2004;291:79–91.
32. Pende D, Marcenaro S, Falco M, Martini S, Bernardo ME, Montagna D, et al. Anti-leukemia activity of alloreactive NK cells in KIR ligand-mismatched haploidentical HSCT for pediatric patients: evaluation of the functional role of activating KIR and redefinition of inhibitory KIR specificity. Blood 2009;113:3119–29.
33. Perussia B, Ramoni C, Anegon I, Cuturi MC, Faust J, Trinchieri G. Preferential proliferation of natural killer cells among peripheral blood mononuclear cells cocultured with B lymphoblastoid cell lines. Nat Immun Cell Growth Regul 1987;6:171–88.
34. Villanueva J, Lee S, Giannini EH, Graham TB, Passo MH, Filipovich A, et al. Natural killer cell dysfunction is a distinguishing feature of systemic onset juvenile rheumatoid arthritis and macrophage activation syndrome. Arthritis Res Ther 2005;7:R30–7.
35. Borhis G, Ahmed PS, Mbiribindi B, Naiyer MM, Davis DM, Purbhoo MA, et al. A peptide antagonist disrupts NK cell inhibitory synapse formation. J Immunol 2013;190:2924–30.
36. Fadda L, Borhis G, Ahmed P, Cheent K, Pageon SV, Cazaly A, et al. Peptide antagonism as a mechanism for NK cell activation. Proc Natl Acad Sci U S A 2010;107:10160–5.
37. Serwold T, Gaw S, Shastri N. ER aminopeptidases generate a unique pool of peptides for MHC class I molecules. Nat Immunol 2001;2:644–51.
38. Sidney J, Peters B, Frahm N, Brander C, Sette A. HLA class I supertypes: a revised and updated classification. BMC Immunol 2008;9:1.
39. Falk K, Rotzschke O, Grahovac B, Schendel D, Stevanovic S, Gnau V, et al. Allele-specific peptide ligand motifs of HLA-C molecules. Proc Natl Acad Sci U S A 1993;90:12005–9.
40. Chelvanayagam G. A roadmap for HLA-A, HLA-B, and HLA-C peptide binding specificities. Immunogenetics 1996;45:15–26.
41. Yan J, Parekh VV, Mendez-Fernandez Y, Olivares-Villagomez D, Dragovic S, Hill T, et al. *In vivo* role of ER-associated peptidase activity in tailoring peptides for presentation by MHC class Ia and class Ib molecules. J Exp Med 2006;203:647–59.

Published OnlineFirst January 15, 2015; DOI: 10.1158/0008-5472.CAN-14-1643

42. Cifaldi L, Romania P, Lorenzi S, Locatelli F, Fruci D. Role of endoplasmic reticulum aminopeptidases in health and disease: from infection to cancer. Int J Mol Sci 2012;13:8338–52.
43. Zervoudi E, Saridakis E, Birtley JR, Seregin SS, Reeves E, Kokkala P, et al. Rationally designed inhibitor targeting antigen-trimming aminopeptidases enhances antigen presentation and cytotoxic T-cell responses. Proc Natl Acad Sci U S A 2013;110:19890–5.
44. van Endert PM, Riganelli D, Greco G, Fleischhauer K, Sidney J, Sette A, et al. The peptide-binding motif for the human transporter associated with antigen processing. J Exp Med 1995;182:1883–95.
45. Testi M, Andreani M, Locatelli F, Arcese W, Troiano M, Battarra M, et al. Influence of the HLA characteristics of Italian patients on donor search outcome in unrelated hematopoietic stem cell transplantation. Tissue Antigens 2014;84:198–205.
46. Hammer GE, Gonzalez F, James E, Nolla H, Shastri N. In the absence of aminopeptidase ERAAP, MHC class I molecules present many unstable and highly immunogenic peptides. Nat Immunol 2007;8:101–8.
47. Ruggeri L, Capanni M, Urbani E, Perruccio K, Shlomchik WD, Tosti A, et al. Effectiveness of donor natural killer cell alloreactivity in mismatched hematopoietic transplants. Science 2002;295:2097–100.
48. Locatelli F, Pende D, Mingari MC, Bertaina A, Falco M, Moretta A, et al. Cellular and molecular basis of haploidentical hematopoietic stem cell transplantation in the successful treatment of high-risk leukemias: role of alloreactive NK cells. Front Immunol 2013;4:15.
49. Mentlik James A, Cohen AD, Campbell KS. Combination Immune Therapies to Enhance Anti-Tumor Responses by NK Cells. Front Immunol 2013;4:481.
50. Chen D, Frezza M, Schmitt S, Kanwar J, Dou QP. Bortezomib as the first proteasome inhibitor anticancer drug: current status and future perspectives. Curr Cancer Drug Targets 2011;11:239–53.

Published OnlineFirst January 15, 2015; DOI: 10.1158/0008-5472.CAN-14-1643

Cancer Research
The Journal of Cancer Research (1916–1930) | The American Journal of Cancer (1931–1940)

AACR American Association for Cancer Research

ERAP1 Regulates Natural Killer Cell Function by Controlling the Engagement of Inhibitory Receptors

Loredana Cifaldi, Paolo Romania, Michela Falco, et al.

Cancer Res 2015;75:824-834. Published OnlineFirst January 15, 2015.